

Magnetoresistance calculations for a two-dimensional electron gas with unilateral short-period strong modulation

Karel Výborný*

I. Institute of Theoretical Physics, University of Hamburg, Jungiusstrasse 9, D-20355 Hamburg, Germany

Ludvík Smrčka

Institute of Physics, Academy of Sciences of the Czech Republic, Cukrovarnická 10, 16253 Praha, Czech Republic

Rainer A. Deutschmann†

Walter Schottky Institut, Technische Universität München, D-85748 Garching, Germany

(Received 28 May 2002; published 21 November 2002)

The linear response theory is used to describe magnetoresistance oscillations of short-period unilateral superlattices with strong modulation (or alternatively arrays of coupled quantum wires). The semiclassical description of this system fails for strong magnetic fields (magnetic breakdown) and we employ a simple fully quantum-mechanical tight-binding model (owing to the fact that coupling between two neighboring wires is much smaller than the height of barrier between them) in conjunction with Kubo's formula instead. The resulting magnetoresistance data nicely compare to the experiments while the model opens good intuitive insight into the effects taking place in the system.

DOI: 10.1103/PhysRevB.66.205318

PACS number(s): 73.63.Nm

I. INTRODUCTION

Transport properties of two-dimensional electron systems (2DES) with unidirectional periodical modulation have been studied for more than ten years. Lot of attention has been paid to the case of weak modulation by electric and magnetic fields. Such a system was first prepared by means of holographic techniques by Weiss *et al.*¹ and showed the commensurability oscillations in magnetoresistance for low magnetic fields and Shubnikov–de Haas (SdH) oscillations for high magnetic fields. Periodicity of the former ones can be well understood even in a semiclassical (SC) concept considering the drift of the cyclotron orbit center in crossed electric and magnetic fields. This approach can also give some quantitative predictions for the magnetoresistance.² An alternative formulation of the SC approach³ relying on the breakdown probability (tunneling between two closed SC orbits) oscillations is also possible. Gerhardt *et al.*⁴ diagonalised the quantum-mechanical (QM) Hamiltonian (and employed the Kubo formula to compute conductivity) finding the oscillating width of Landau bands (Landau levels broadened by the weak modulation into narrow cosine-like bands) to be the basic cause of the effect within the QM picture. QM approach was also applied by Vasilopoulos *et al.*⁵

The SdH oscillations follow naturally from the QM concept owing to the quantization of free electron motion in magnetic fields [Landau levels (LL's)]. This quantization has to be *ad hoc* assumed in the SC picture but once this is accepted, the SC theory provides a sufficient description in this case.

Experiments on gated structures manufactured by lithographic techniques performed by Beton *et al.*⁶ allowed for investigating effects of stronger modulation. Compared to the previously mentioned experiments, the major effect was the quenching of the commensurability oscillations. The SC approach² was applicable again,⁶ although quantum

calculations⁷ were in better agreement with experiments. Later, the SC theories have been extended in order to account for anisotropic scattering⁸ and for modulation by magnetic field^{9,10} (extending the older works^{2,11}). For QM approach to modulation by magnetic field see e.g.,¹² All together, the SC approach proved itself to be suitable in these cases.

More recently, samples with modulation potential due to MBE-grown structure were prepared (using cleaved edge overgrowth technique) by Deutschmann *et al.*¹³ In contrast to all former experiments, the modulation period $d = 15$ nm was shorter by almost one order of magnitude. Owing to this fact and also due to strong modulation (Fermi energy $E_F \approx 4|t| \ll V_0$, where t is the hopping integral between ground states in two neighboring wells of the potential modulation and V_0 is the height of barriers³⁰ between those wells, see Fig. 1), the lowest modulation miniband is well separated from higher minibands [the condition for this is $d \lesssim \sqrt{3\hbar^2/(2|t|m)}$]. The magnetoresistance oscillations measured when the Fermi level lies between the modulation bands can be explained by no semiclassical model unless tunneling between open trajectories is assumed (the breakdown formalism³ mentioned above is necessary at this place). It is thus appropriate to revert to a quantum-mechanical description. Moreover, the miniband structure is simple now and allows thus for a good insight into the physics both on the SC and quantum-mechanical level.

The cleaved edge overgrowth technique is not the only way to produce unilaterally modulated 2DES with short modulation period. Also recently, Iye *et al.*¹⁴ reported on magnetoresistance measurements on samples with modulation period as short as 12 nm. In these experiments, 2DES is located near to a GaAs/AlAs interface where there are regular steps on the GaAs (775)B surface [which is slightly tilted to the (111) plane]. The effective potential modulation of the 2DES due to the steps seems to be weak and thus our model

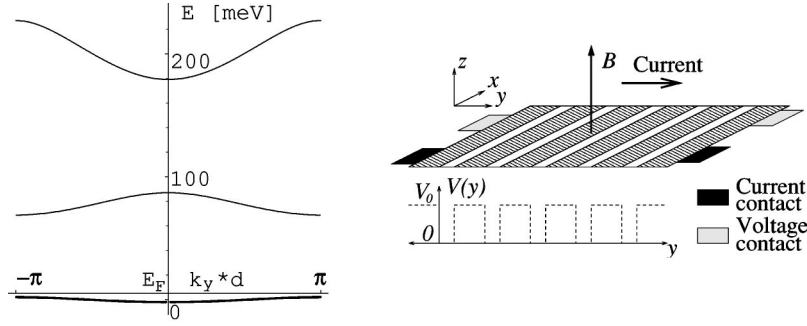


FIG. 1. Right: 2DES with lateral periodical modulation and the effectively two-point-contact geometry. Alternatively, this may be conceived as an array of coupled quantum wires (parallel to the x axis). The “wires” (layers of GaAs) and the “barriers” (layers of $\text{Al}_x\text{Ga}_{1-x}\text{As}$, $x=0.32$) were 11.9 and 3.1 nm thick in the experiments (Ref. 13) we refer to. Owing to the height of the “barriers” the coupling between wires is small ($E_F \approx 4|t| \ll V_0$) and a tight-binding model is thus appropriate. Left: Zero field band structure (along k_y) calculated by Kronig-Penney model. We keep only the lowest band (thick line) in our calculations and we set $4|t|$ equal to the width of this band.

is not relevant for these experiments. Other experiments were presented by Chowdhury *et al.*¹⁵ who fabricated bilaterally modulated systems with modulation periods around 100 nm using electron beam lithography followed by shallow wet etching.

The structure of this paper is the following. At the beginning we will review the semiclassical approach as a favorite tool used to describe magnetotransport experiments. We will also compare the zero-field density of states (DOS) with the $B \neq 0$ DOS computed in Sec. II. It will give us illustrative examples of a situation when the SC theory is expected to be successful and of another situation when it should fail. The condition of applicability of the SC approach will be shown to be $\hbar\omega_{\text{eff}} \ll 2|t|$ whereas $\omega_{\text{eff}} = eB/m_{\text{eff}} = eB/\sqrt{mm_y}$.

In the second part (Sec. II) we will describe a fully quantum-mechanical one-particle model and demonstrate that the gaps in the DOS emerging from this model coincide with extrema in the measured magnetoresistance. Then we will employ the linear response theory (Sec. III) in order to calculate the magnetoresistance and we will compare it with the experiments.

A. The system

In this paper, we refer to experiments carried out on GaAlAs/GaAs structures first reported in Ref. 13, see also more detailed description in Refs. 16,17. These are superlattices with strong unilateral short-period (electric-field) modulation. The substantial difference to previous studies (see the Introduction) is the shortness of the modulation period: only the lowest modulation band (and not many of them) is occupied under those circumstances which makes the usage of quantum mechanics inevitable. Moreover, absence of the higher modulation bands makes the model very transparent. We concentrate on magnetoresistance measurements at different concentrations of electrons (which could be varied by a gate voltage over the range $0.5\text{--}5.0 \times 10^{11} \text{ cm}^{-2}$). The system is sketched in Fig. 1.

The miniband structure in zero magnetic field calculated within the Kronig-Penney model (see also Fig. 1) can be well approximated by

$$E(k_x, k_y) = \frac{\hbar^2 k_x^2}{2m} - 2|t| \cos k_y d \quad (1)$$

with $4|t| \approx 3.8 \text{ meV}$ and m equal to the effective mass of electrons in GaAs. The next modulation band is well above the Fermi level E_F for all accessible concentrations. The first and the second modulation band are separated by $\approx 60 \text{ meV}$ according to the Kronig-Penney model.

If the Fermi level lies near the bottom of the band ($-2|t| < E_F \ll 2|t|$), the system resembles a free 2DES (i.e., paraboloidal spectrum with modified effective mass in the modulation direction $m_y = \hbar^2/2|t|d^2 \approx 2.7m$). If the Fermi level lies high above the modulation band edge ($E_F \gg 2|t|$), the dispersion relation is similar to the one of an array of separated one-dimensional wires (i.e., parabolic across k_x and nearly constant along k_y) while the deviation from $E = \hbar^2 k_x^2/2m$ reflects the coupling of wires.

B. Semiclassical approach

The physical quantity of central importance in transport theories is the density of states $g(E)$ (DOS) at the Fermi level E_F . It is known that its structure reflects features of the resistance (both as a function of B , for instance) but the relation between these two quantities is not simple.

The SC theory attempts to explain the behavior of electrons subject to a magnetic field in terms of the zero-field Fermi surfaces. We demonstrate that the zero-field DOS plus an extra quantization condition is a fairly good approximation to the realistic DOS (computed by our model, from Sec. II) at low magnetic fields ($\hbar\omega_{\text{eff}} \ll 2|t|$). However, there is a drastic difference between these two densities of states for high magnetic fields indicating failure of the SC theory (see Fig. 3).

Let us briefly review the SC approach suggested by Lifshitz and Onsager (see, e.g., Ref. 18). We construct the Fermi contour $E_F = E(k_x, k_y)$ for a given Fermi level. The statements are that (1) the Fermi contour rotated by 90° and scaled by $l^2 = \hbar/eB$ corresponds to the real-space trajectory of an electron (see Fig. 2) and (2) if the contour is closed, then it is allowed only if the magnetic flux passing through

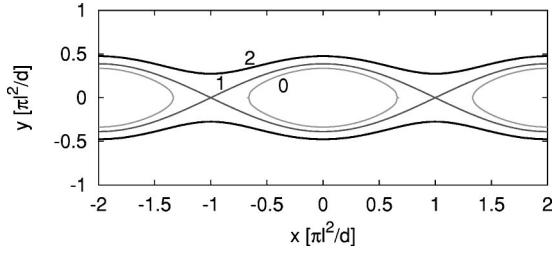


FIG. 2. Real-space semiclassical trajectories of electron in magnetic field. 0: closed ($E_F < 2|t|$), 1: critical ($E_F = 2|t|$), 2: open ($E_F > 2|t|$). The closed trajectories are elongated in the direction parallel to the wires by a constant factor $\sqrt{m_y/m}$ and due to non-parabolicity of the cosine band [Eq. 1].

the area enclosed by the real-space trajectory is an integer multiple of the magnetic flux quantum $\Phi_0 = h/e$. In the QM picture, this quantization condition corresponds to the situation when $E_F = \hbar \omega_{\text{eff}}(n + \frac{1}{2})$ for some integer n , i.e., when the n th LL passes through the Fermi level.

So as to be able to compare the SC and QM predictions let us now examine the densities of states. Note that by comparing the zero-field DOS of our system (for $E \ll 2|t|$, i.e., in the region of quantized orbits and 2D-like behavior) with the zero-field DOS of a free 2DES [$g(E) = 2m_{\text{eff}}/\pi\hbar^2$ including spin] we may deduce the modulation-influenced effective mass m_{eff} . This in turn determines the quantization condition $E_F = \hbar \omega_{\text{eff}}(n + \frac{1}{2})$ and thus all SC predictions can be made using the zero-field DOS of the system only. Based on the spectrum [Eq. (1)] we can compute the zero-field DOS analytically

$$g_0(E) = \begin{cases} \frac{4}{(2\pi)^2} \sqrt{\frac{2m}{\hbar^2|t|d^2}} \frac{1}{\sqrt{\xi}} K(1/\sqrt{\xi}), & E > 2|t|, \\ \frac{4}{(2\pi)^2} \sqrt{\frac{2m}{\hbar^2|t|d^2}} K(\sqrt{\xi}), & -2|t| < E < 2|t|, \end{cases} \quad (2)$$

where

$$\xi = \frac{1 + E/2|t|}{2}$$

including the factor of 2 for spin (the dotted line in Fig. 3). K is the full elliptic function $K(k) = F((\pi/2), k) = \int_0^{\pi/2} (1 - k^2 \sin^2 \varphi)^{-1/2} d\varphi$, we recall¹⁹ that $K(0) = \pi/2$, $K(1) = \infty$.

Let us focus on the weak-field case first ($\hbar \omega_{\text{eff}} \ll 2|t|$) and discuss the influence of magnetic field B on the continuous spectrum [Eq. (1)], i.e. we try to estimate the DOS in magnetic fields without any calculation. On one hand, Landau levels (LL's) appear for $E_F \ll 2|t|$ (2D-like paraboloid band structure, modified effective mass m_y). If the thermal energy is comparable to the Landau level separation ($k_B T \approx \hbar \omega$) the DOS becomes oscillatory (leading to SdH oscillations) but approaches the zero-field DOS (see also Fig. 3). In other words, the oscillations missing in the zero-field DOS are

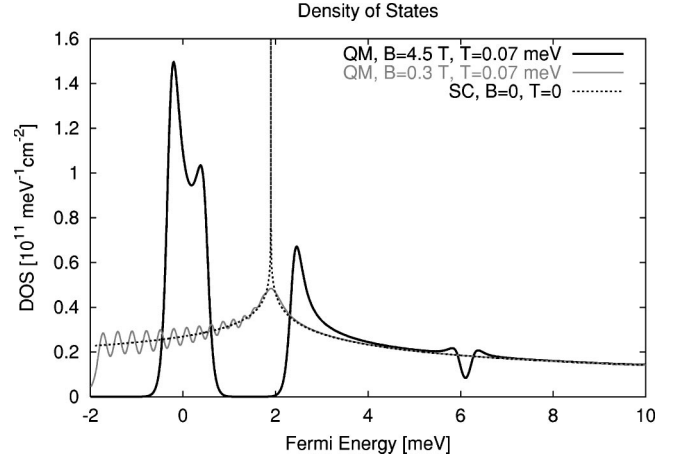


FIG. 3. The density of states for $B=0$ (dotted) and thermally broadened ($T \approx 1$ K) density of states for low field ($\hbar \omega_{\text{eff}} \ll 2|t|$ or $\alpha \ll 1$, solid gray line) and high field (solid black line).

exactly reproduced by the SC quantization condition (closed trajectories, $E_F < 2|t|$) which is fulfilled just when E_F lies in the middle between two LL's.

On the other hand, narrow gaps open in the continuous spectrum for $E_F \gg 2|t|$ due to the slight corrugation (by the cosine term) of the almost 1D-like parabolic-trough band structure. Numerical calculations (using model from Sec. III) show that these gaps are narrow enough to disappear due to thermal broadening and the zero-field DOS matches the nonzero-field DOS perfectly. The SC approach relying on non-quantized open trajectories ($E_F > 2|t|$) and predicting nonscillatory magnetoresistance will therefore be successful once again.

The picture is considerably different for strong magnetic fields ($\hbar \omega_{\text{eff}} \geq 2|t|$) at which the cyclotron radius R_c approaches d . The numerically computed DOS shows no similarity to the zero-field DOS (Fig. 3 again). The nonzero-field DOS rather resembles $g(E) \propto 1/\sqrt{E}$ of a single quantum wire (suppression of tunneling between two neighboring wires when classical cyclotron radii become comparable to d) with gaps both for $E < 2|t|$ and $E > 2|t|$ owing to the tunneling between the wires. Therefore we expect oscillatory magnetoresistance for both closed and open SC trajectories on contrary to the SC predictions (magnetic breakdown in the SC theory).

The gaps occur at the boundary of the first magnetic Brillouin zone (1MBZ) (see Sec. II) and result from the periodicity of the dispersion relation in k_x which in turn reflects the invariance of the QM Hamiltonian to magnetic translations²⁰ (this is what remains from the full translational symmetry in the x direction after switching on the magnetic field). Magnetic breakdown can be included also in the SC picture through tunneling between two open or two closed trajectories³ (see Fig. 2). This is an *ad hoc* assumption though.

The failure of the SC approach for strong magnetic fields is apparent also in another context. Once the Fermi level is set and the type of trajectory is determined, the same behavior (either 2DES-like SdH oscillations or 1DES-like no oscillations) is predicted for all magnetic fields. However, it is

clear even on the SC level that if the cyclotron radius $R_c = k_F l^2$ (k_F is the Fermi wave vector, $E = \hbar^2 k_F^2 / 2m$) becomes comparable to d , tunneling between the wires is suppressed and the system ought to switch to a quasi-1D regime.

The QM approach is suitable for both low and strong magnetic fields. Moreover, it opens up the way to quantitative calculations of the magnetoresistance and thus to data directly comparable to the experiments.

II. MODEL

Having chosen the Landau gauge $\vec{A} = (By, 0, 0)$ our system is described by the separable Hamiltonian ($e = |e|$)

$$H = \frac{1}{2m} (p_x + eBy)^2 + \frac{1}{2m} p_y^2 + V(y), \quad (3)$$

i.e., allowing to set $\Psi(x, y) = \exp(ikx)\psi(y)$ for the eigenfunctions. Our ansatz for the whole wave function is

$$\Psi(x, y) = \frac{1}{\sqrt{2\pi}} \exp(ikx) \sum_j a_j(k) \varphi(y - jd), \quad (4)$$

i.e., we use the ansatz $|\psi(k, n)\rangle = \sum_j a_j(k) |j\rangle$ for $\psi(y)$ [n is the Landau index in the spectrum of Eqs. (5) or (3) for a given k] where $|j\rangle$ is the ground state localized in the j th well of the potential (corresponds to the Wannier state of the $B=0$ case). We have thus limited our model just to the lowest band in the modulation direction by this ansatz. The Fermi level lies always deep below the top of the modulation potential in our calculations.

Next we use the tight-binding approximation (i.e., $\langle i|j\rangle = \delta_{i,j}$, $\langle i|H|j\rangle = t\delta_{i,j\pm 1}$, $t < 0$) and obtain the Hamiltonian matrix elements (see also Wulf *et al.*²¹)

$$H_{ij} = \frac{\hbar^2}{2m} K^2 [(k/K) + i]^2 \delta_{i,j} + t \delta_{i,j\pm 1}, \quad K = d \frac{eB}{\hbar}. \quad (5)$$

In our model the real physical system is thus represented by the parameters t (hopping) and d (period) for the structure and of course B for the magnetic field.

Note that (up to the scaling of k and energy) the problem (5) effectively depends only on the single parameter α : Eq. (5) can be written in dimensionless form

$$H_{ij} = |t| [\alpha^2 ((k/K) + i)^2 \delta_{i,j} - \delta_{i,j\pm 1}], \quad (6)$$

$$\alpha^2 = \frac{e^2 B^2}{m} \frac{d^2}{2|t|} = \left(\frac{\hbar \omega_{\text{eff}}}{2|t|} \right)^2.$$

If we now assume the system to be infinite in the y direction the matrix problem (5) is mathematically equivalent to the Mathieu equation

$$-\frac{\hbar^2}{2m} \psi''(x) - 2|t| \cos(Kx) \psi(x) = E \psi(x), \quad (7)$$

i.e., 1D Schrödinger equation for a fictitious particle subjected to potential $W(x) = -2|t| \cos Kx$. The detailed description of this model can be found in Ref. 22. To avoid misunderstanding, let us point out that the amplitude of $W(x)$ and

the height of the barriers between the wires (see Fig. 1) are different quantities, moreover if V_0 grows, the amplitude of $W(x) \propto 2|t|$ falls.

This allows us to determine the spectrum of Eq. (5) qualitatively, and therefore also the DOS, even before we carry out the numerical calculations. Let the magnetic field be weak at first ($\alpha \ll 1$, see explanation below in this paragraph). Bands $E(k)$ should appear (as a consequence of the Bloch theorem) and we may limit ourselves to 1MBZ, the first “magnetic Brillouin zone” $k \in (-\frac{1}{2}K, \frac{1}{2}K)$. For $E \ll 2|t|$ we expect those bands to be equidistantly spaced and narrow. The former follows from $W(x) \approx 2|t|(-1 + \frac{1}{2}K^2 x^2)$ near the potential minimum (the condition $\alpha \ll 1$ means just that the spacing of such states is $\ll 2|t|$), the latter is due to the smallness of the overlap of low-lying states in two neighboring wells of $W(x)$. In contrast, for $E \gg 2|t|$ we expect the spectrum to be almost similar to the one of 1D free electrons $E(k) = \sum_i \hbar^2 (k + iK)^2 / 2m$. The underlying nonconstant potential V will manifest itself in the gaps which open at the Brillouin zone boundaries ($k = \pm \frac{1}{2}K$).

Let us now translate this analysis into terms of the original problem (5). Consider a fixed magnetic field (or constant α). For low energies we obtain nearly equidistant and sharp Landau levels (free 2D electron gas in magnetic field). At high energies we get a sum of almost 1D densities of states, i.e. independent quantum wires (where B plays no role). The transition occurs around $E = 2|t|$. This agrees with the semiclassical theory except for the narrow gaps in the continuous quasifree-1D-electron part of the spectrum. These indicate the magnetic breakdown for quantizing magnetic fields.

Secondly, we focus on strong magnetic fields ($\alpha \gg 1$). On one hand, the states of Eq. (7) below $2|t|$ will become more widely spaced and even the lowest state will no longer have $E \ll 2|t|$. We then expect even the lowest LB to be broad (solid black curve at Fig. 3) because its energy lies in an intermediate region between $E \ll 2|t|$ and $E \gg 2|t|$. On the other hand, the states with $E > 2|t|$ which approach the free electron states (and have a nearly free-electron parabolic spectrum) will have wider gaps (the smaller the lattice constant of a crystal, the wider the gaps).

We may now compare the DOS being output from our model with the experimentally measured resistance, see Fig. 4. In the experiments, the Fermi energy was adjusted by applying a gate voltage U_g and we assume that E_F remains constant while magnetic field is swept. Literally taken, this would imply that the electron concentration N in the 2DES is not constant but oscillates with B . To be able to keep both E_F and N constant consistently within our model we use the zero-field relation between E_F and N . This may be conceived as an effect of localization (which is necessary for the Hall plateaus to be visible, see Fig. 4).

Experiments showed that the concentration of electrons is proportional to the gate voltage (see Sec. IV). The proportionality constant is also approximately equal to the capacity of a parallel-plate capacitor corresponding to the gated structure. Looking at Fig. 4 we see the gaps in the DOS matching very well with the straight lines of magnetoresistance extrema which justifies the $U_g \leftrightarrow E_F \neq E_F(B)$ model of ours.

We can see in the Fig. 4 that varying the magnetic field

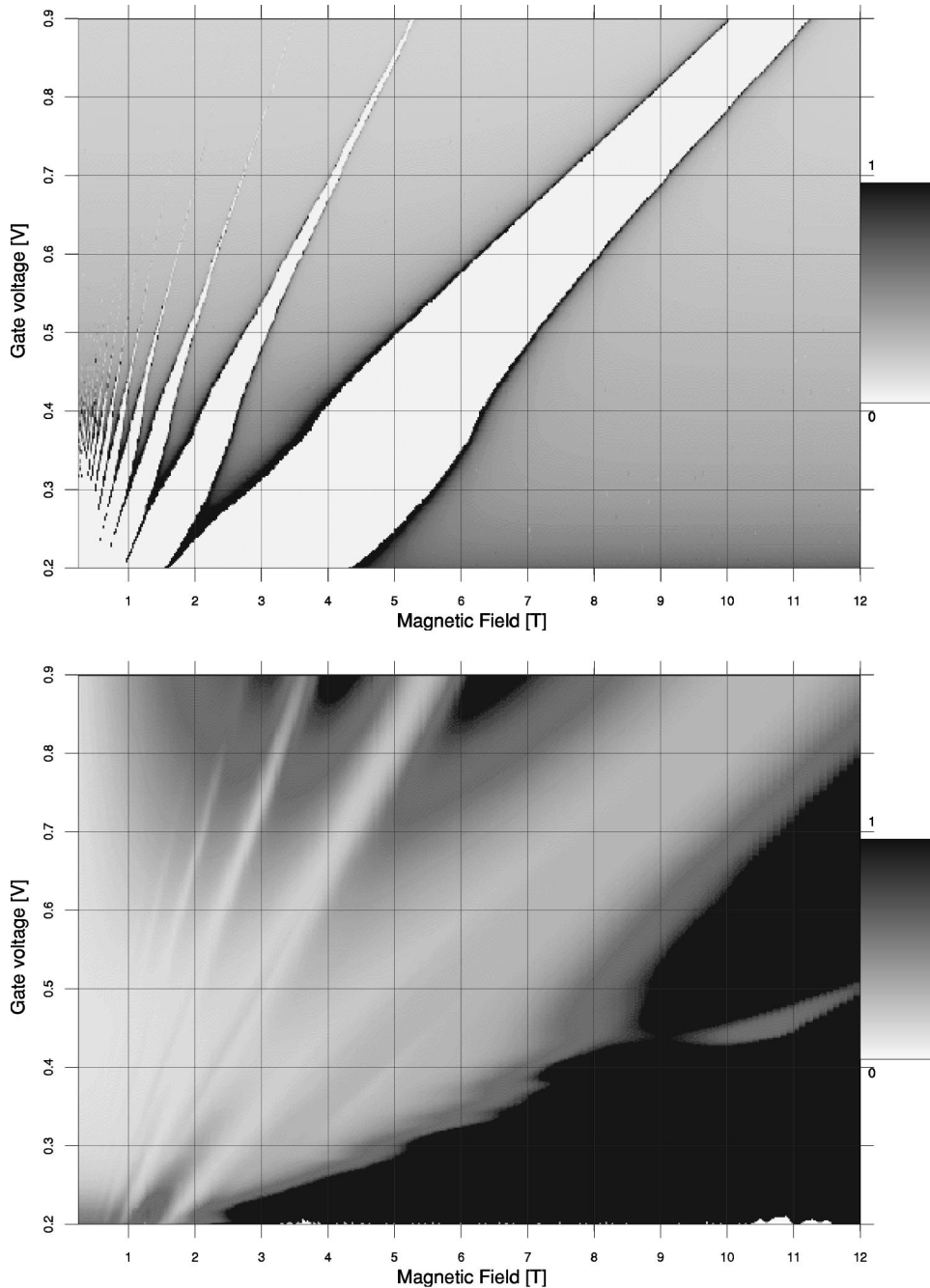


FIG. 4. Above: density of states (arbitrary units) in the tight-binding model for different magnetic fields and gate voltages. Below: measured resistance (logarithmic scale in the shade code, arbitrary units). Note the match between the gaps in the DOS (light stripelike regions) and the extrema in the magnetoresistance (usually light regions of shapes similar to the former ones).

and keeping the Fermi energy (or U_g) constant and low the system behaves like an almost free 2D electron gas (sharp LL's, equidistant in $1/B$) with modified effective mass $\sqrt{m m_y}$ (as predicted by SC theory). At intermediate E_F , however, we observe that the narrow bands become broad at high B indicating an effective 2D to 1D transition (when cyclotron radii become smaller than the modulation period). In contrast, the SC theory states that once the Fermi energy is set, a magnetic field cannot change the dimensionality of the system. When E_F is high the quantum wires are decoupled, but there still open gaps in the continuous spectrum (reflecting the tunneling between the open SC orbits).

The lighter region around $B \approx 11$ T and $U_g \approx 0.45$ V in the experimental data (Fig. 4 below) suggests that our model

works no longer for strong magnetic fields ($\alpha \gg 1$) and low Fermi energies (even the lowest LB nearly empty). This condition matches the situation when the cyclotron radius is much smaller than d and it means that our tight-binding model is inappropriate for magnetic fields strong enough to create LLs within one quantum wire (so that even the width of wires will be large enough for the electrons to behave as a 2DES inside one wire). These are, however, rather extreme conditions for the experiments shown in Fig. 4.

III. TRANSPORT: KUBO FORMULA

Knowing the eigenfunctions to the matrix problem (5) we may use the linear response theory (Kubo formula, see e.g.

Ref. 23) to compute the conductivity tensor components (per system area A)

$$\begin{aligned}\sigma_{ii}(E_F) &= \frac{\pi\hbar e^2}{A} \text{Tr}[\hat{v}_i \delta_\Gamma(E_F - \hat{H}) \hat{v}_i \delta_\Gamma(E_F - \hat{H})] \\ \sigma_{xy}(E) &= \frac{i\hbar e^2}{A} \cdot \frac{1}{2} \text{Tr}[\hat{v}_x \hat{G}^+(E) \hat{v}_y \delta_\Gamma(E - \hat{H}) \\ &\quad - \hat{v}_x \delta_\Gamma(E - \hat{H}) \hat{v}_y \hat{G}^-(E)] + e \frac{\partial N(E)}{\partial B}.\end{aligned}$$

Here $\hat{v}_{x,y}$ stand for the velocity operator components, $\delta_\Gamma(E - \hat{H}) = -(1/2\pi i)[\hat{G}^+(E) - \hat{G}^-(E)]$ and $\hat{G}^\pm(E) = (E - \hat{H} \pm i\Gamma)$. Isotropic scattering by a random impurity potential is taken into account by means of the complex-valued self-energy $\Sigma = \Delta + i\Gamma$ and we neglect its real part. In the self-consistent Born approximation and assuming $\Gamma(E, B)$ to be small compared to the level separation (typically $\hbar\omega_{\text{eff}}$) we can express components of σ by means of the DOS $g(E)$ and matrix elements of y ($\omega = eB/m$)

$$\begin{aligned}\sigma_{xx}(E) &= \frac{2}{\pi\Gamma d} \frac{e^2}{\hbar} \frac{\text{sgn}[g(E)]}{g(E)} + \frac{4\pi\Gamma}{d} (\hbar\omega)^2 \frac{e^2}{\hbar} g(E) \\ &\quad \times \sum_{n' \neq n} \left(\frac{\langle \psi(k, n') | y | \psi(k, n) \rangle}{E(k, n') - E(k, n)} \right)^2, \\ \sigma_{yy}(E) &= \frac{4\pi\Gamma}{d} \frac{e^2}{\hbar} g(E) \sum_{n' \neq n} (\langle \psi(k, n') | y | \psi(k, n) \rangle)^2, \\ \sigma_{xy}(E) &= e \frac{\partial N(E)}{\partial B} + \frac{4\pi\hbar\omega}{d} \frac{e^2}{\hbar} g(E) \\ &\quad \times \sum_{n' \neq n} (\langle \psi(k, n) | y | \psi(k, n') \rangle)^2\end{aligned}$$

(including spin degeneracy). The symbolic expression $\text{sgn}[g(E)]/g(E)$ in the first term of σ_{xx} indicates that this term vanishes if $g(E) = 0$. Just to get simpler formulas, the additional assumption has been made that there are merely two points at the Fermi level $E = E(k, n)$ within the 1MBZ. We reproduced the older results of Wulf *et al.*²¹ where the Γ -independent $\sigma_{xy}(E)$ was calculated within the same model but in a formally different way [Eqs. (5),(6) in Ref. 23].

Note the structure of the components of σ : in general, all the terms (except for the $\partial N/\partial B$ term in σ_{xy}) are products of the DOS (g) and some matrix elements of \hat{y} . There are two contributions to the conduction parallel to the wires (σ_{xx}): the first term (proportional to $1/g$) originates from the diagonal matrix elements $\delta(k - k') \hbar k / (eB) + \langle \psi(k', n) | \hat{y} | \psi(k, n) \rangle \propto \langle \psi(k', n) | \hat{v}_x | \psi(k, n) \rangle = (1/\hbar)(dE/dk) \delta(k - k') \propto 1/g$. It corresponds to the classical conductivity of a wire (open electron trajectories) or in other words it does not vanish owing to the unilateral modulation, of the system: without modulation (free 2DES) the DOS comprises of delta peaks (sharp LL's) and $(\text{sgn } g)/g \rightarrow 0$. For $E < 2|t|$, we ob-

tain from our calculations LBs with nonzero width and this reflects tunneling between two closed orbits in the SC picture (see Fig. 2), i.e., indicates a deviation from the quasi-2D behavior. This contribution to conductivity is being *suppressed* by the impurity scattering (by $1/\Gamma$) or in other words, persists even if there is no impurity scattering at all.

The conduction perpendicular to the wires (σ_{yy}) and the second term of σ_{xx} reflect the inter-LB transitions and appear thus *due to* impurity scattering (they are proportional to Γ). These contributions might be viewed as a consequence of tunneling between the open SC orbits. There is no requirement that $\langle \psi(n, k) | y | \psi(m, k) \rangle = 0$ for $|n - m| > 1$ as in the limit of weak modulation, but we found these matrix elements to be decaying rapidly with growing $|n - m|$. In other words, inter-LB scattering occurs dominantly between neighboring LB's. The Hall conductivity does not depend on the scattering in the leading order at all.

Let us now concentrate on the issue of impurity scattering. Following Refs. 20,24,25 we used an ansatz of self-energy depending only on energy (and B). This leads to a self-consistent equation

$$\Sigma(E) \propto \text{Tr} \frac{1}{E - H - \Sigma(E)},$$

where the proportionality constant describes the strength of the impurity scattering. This equation yields^{26,27} the well-known result

$$\Gamma^2 = \frac{1}{2\pi} \hbar \omega \frac{\hbar}{\tau}$$

for free 2DES (i.e., no modulation) and short-range scattering potential. τ is the relaxation time in the zero magnetic field case (as in the Drude theory). In our calculations we used this (i.e., $\Gamma = \gamma\sqrt{B}$) as a phenomenological ansatz which has already proven to be useful in explaining the magnetoresistance data by long-period superlattices.^{28,29} Surprisingly enough, even this simple ansatz provides a very good qualitative agreement with the experimental data and makes the results of the calculations depend on the fitting parameter (γ , scattering strength) in a very simple way.

In order to obtain data comparable to experiments, we need to express the resistivity tensor components

$$\varrho_{yy} = \frac{\sigma_{xx}}{\sigma_{xx}\sigma_{yy} + \sigma_{xy}^2}, \quad \varrho_{xy} = \frac{\sigma_{xy}}{\sigma_{xx}\sigma_{yy} + \sigma_{xy}^2}. \quad (8)$$

A remarkable and important point of these formulas is that if scattering is weak (i.e., the inter-LB term $\propto \Gamma$ in σ_{xx} may be neglected), the denominators do not depend on Γ .

Due to the particular sample geometry a two-point measurement is performed and thus the experimentally accessible quantity is $R_{yy} + R_{xy}$ (longitudinal and transversal resistance in series). Here $R_{xy} = \varrho_{xy}$ and $R_{yy} = c\varrho_{yy}$ with some dimensionless constant geometrical factor c . Thus it seems plausible to assume that the voltage drop measured is a constant linear combination of ϱ_{xy} and ϱ_{yy}

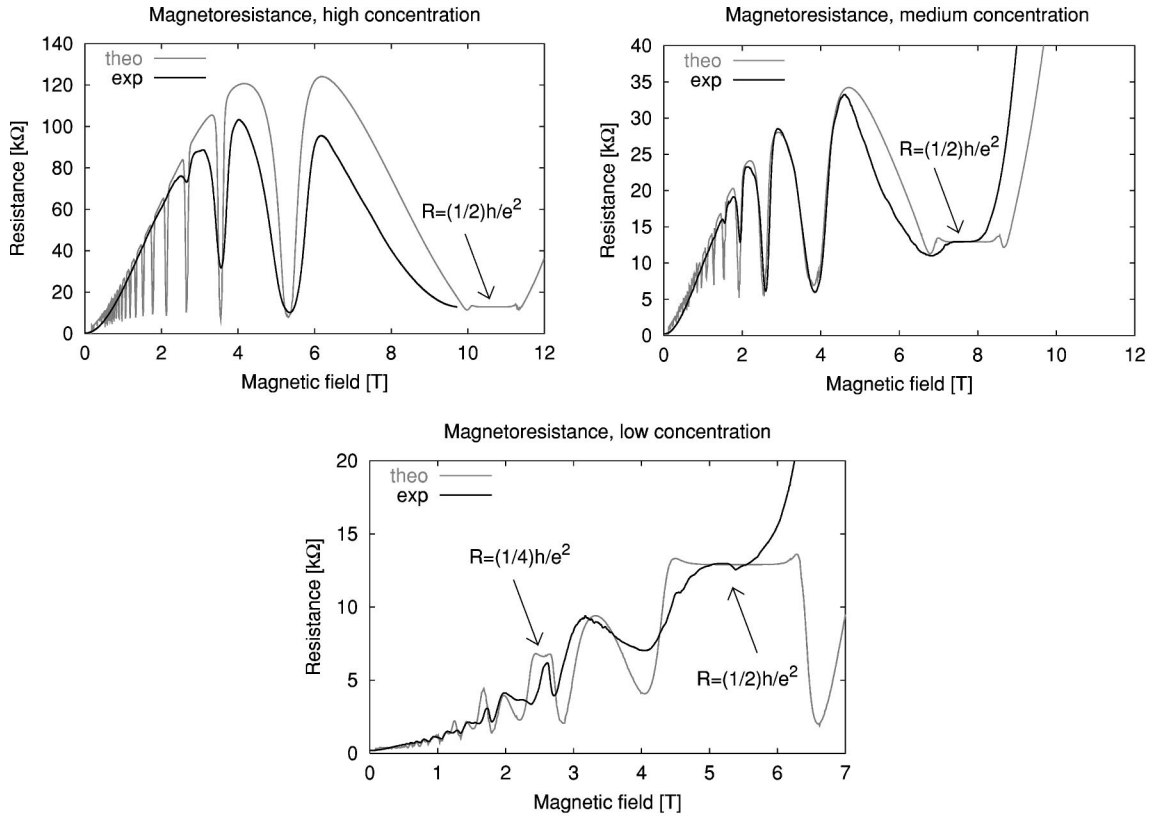


FIG. 5. Magnetoresistance. Calculations and experiment. Electron concentrations (from the top) $5.1 \times 10^{11} \text{ cm}^{-2}$, $3.8 \times 10^{11} \text{ cm}^{-2}$, $2.65 \times 10^{11} \text{ cm}^{-2}$. The lowest concentration corresponds to $E_F \approx 2|t|$.

$$R = c \varrho_{yy} + \varrho_{xy}.$$

If scattering is weak, the magnetoresistances to be compared to experimental data contain a single fitting parameter c/γ . This comparison for different electron densities is shown in Fig. 5.

IV. DISCUSSION

Almost quantitative agreement is achieved for high concentrations [Figs. 5(a), 5(b)]. Exact (no fitting parameter) match between the magnetoresistance extrema in theory and experiments (which has been emphasised already on the DOS level) shows that the tight-binding model captures the essential physics in our experiments.

Note also that the magnetoresistance approaches quantized values $R = (1/\nu)h/e^2$ for E_F lying in the gap. First, this allows us to determine the concentration of electrons N in the system (compare filling factor of each plateau ν and its B). Second, it confirms our model of the relation between the gate voltage U_g and Fermi level E_F . However, as we may see best in Fig. 5(c), there is still room for improving the model, e.g., by taking the localization effects into account.

The quadratic rise of resistivity at low magnetic fields due to the diagonal component (ϱ_{yy}) has been predicted within a SC model² and measured also at weak-modulation samples.²⁹ Our results [with a single fitting parameter in Figs. 5(a), 5(b)] deviate from this slightly because of the form of $\Gamma(E, B) \propto \sqrt{B}$. Assuming Γ independent on B in this region,

the quadratic behavior is reconciled. For intermediate fields the matrix elements of \hat{y} start to play a role.

Another feature of the tight-binding model is the capability of explaining why the Hall plateaus show minima at high concentrations and maxima at low concentrations [Fig. 5(c)]. Note, however, that even at this concentration $E \approx 2|t|$. Swapping the dominance of σ_{xy} and $\sigma_{xx,yy}$ [see Eq. (8)] is the cause for the qualitative change of the magnetoresistance curve. Nevertheless, we are aware of the feebler match between theory and experiments at lower concentrations indicating that our ansatz for the self-energy is rather crude.

V. CONCLUSION

The cleaved-edge-overgrowth technology opens a new area of 2DES with short-period atomically precise unidirectional modulation for experimental studies. Such samples may be viewed as an array of coupled quantum wires which can be decoupled by applying reasonable (≈ 5 T) perpendicular magnetic field. From a theoretical point of view, these systems have a simple band structure and can be very well described by a simple tight-binding model. It was demonstrated that for weak magnetic field ($\hbar\omega_{\text{eff}} \ll 2|t|$) the SC approach arguing with closed and open electron trajectories is expected to be fairly good and it is good indeed. On the other hand, this approach fails for quantizing magnetic fields (magnetic breakdown in the SC terminology). The fully quantum-mechanical tight-binding model offers both a

good way to estimate the applicability of the SC approach and a reasonable description of the system for any magnetic field unless $R_c = k_F l^2 \ll d$. This model is also very intuitive on the level of DOS analysis owing to the analogy with Mathieu equation (7).

We found good agreement between the experimental magnetoresistance and calculations based on the linear response theory even with a very simple model for impurity scattering. We expect that the match between theory and experi-

ment may be improved by internally consistent treatment of scattering due to randomly distributed impurities.

ACKNOWLEDGMENTS

One of the authors (K.V.) would like to acknowledge discussions with Daniela Pfannkuche and Alexander Chudnovskiy. This work has been partly supported by the DFG through Grant SFB508 and by the Grant Agency of the Czech Republic under Grant No. 202/01/0754.

*Electronic address: vybornyk@fzu.cz

[†]Now with McKinsey&Company.

¹D. Weiss, K. von Klitzing, K. Ploog, and G. Weinmann, Europhys. Lett. **8**, 179 (1989).

²C. Beenakker, Phys. Rev. Lett. **62**, 2020 (1989).

³P. Středa and A. MacDonald, Phys. Rev. B **41**, 11 892 (1990).

⁴R. Gerhardt, D. Weiss, and K.v. Klitzing, Phys. Rev. Lett. **62**, 1173 (1989).

⁵P. Vasilopoulos and F. Peeters, Phys. Rev. Lett. **63**, 2120 (1989).

⁶P. Beton, E. Alves, P. Main, L. Eaves, M. Dellow, M. Henini, and O. Hughes, Phys. Rev. B **42**, 9229 (1990).

⁷Q. Shi and K. Szeto, Phys. Rev. B **53**, 12 990 (1996).

⁸R. Menne and R. Gerhardt, Phys. Rev. B **57**, 1707 (1998).

⁹S. Zworschke and R. Gerhardt, Physica B **256**, 28 (1998).

¹⁰S. Zworschke, A. Manolescu, and R. Gerhardt, Phys. Rev. B **60**, 5536 (1998).

¹¹J. Müller, Phys. Rev. Lett. **68**, 385 (1992).

¹²F. Peeters and P. Vasilopoulos, Phys. Rev. B **47**, 1466 (1993).

¹³R.A. Deutschmann, A. Lorke, W. Wegscheider, M. Bichler, and G. Abstreiter, Physica E **6**, 561 (2000).

¹⁴Y. Iye, S. Katsumoto, Y. Ohno, S. Shimomura, and S. Hiyamizu, Physica E **12**, 200 (2002).

¹⁵S. Chowdhury, E. Skuras, C.J. Emeleus, A.R. Long, J. Davies, G. Pennelli, and C.R. Stanley, Phys. Rev. B **63**, 153306 (2001).

¹⁶R.A. Deutschmann, W. Wegscheider, M. Rother, M. Bichler, G.

Abstreiter, C. Albrecht, and J.H. Smet, Phys. Rev. Lett. **86**, 1857 (2001).

¹⁷R.A. Deutschmann, *Two Dimensional Electron Systems in Atomically Precise Periodic Potentials*, Vol. 42 of *Selected Topics of Semiconductor Physics and Technology* (University of Technology, Munich, 2001).

¹⁸N. Ashcroft and N. Mermin, *Solid State Physics* (Saunders College Publishing, Orlando, 1976), p. 232.

¹⁹I. Gradshteyn and I. Ryzhik, *Table of Integrals, Series and Products* (Academic Press, San Diego, 1980), p. 904.

²⁰D. Pfannkuche and R. Gerhardt, Phys. Rev. B **46**, 12 606 (1992).

²¹U. Wulf, J. Kučera, and A. MacDonald, Phys. Rev. B **47**, 1675 (1992).

²²S. Davidson and M. Stęślicka, *Basic Theory of Surface States* (Clarendon Press, Oxford, 1992), p. 41.

²³P. Středa, J. Phys. C **15**, L717 (1982).

²⁴C. Zhang and R. Gerhardt, Phys. Rev. B **41**, 12 850 (1990).

²⁵T. Ando, A. Fowler, and F. Stern, Rev. Mod. Phys. **54**, 437 (1982).

²⁶R. Gerhardt and J. Hajdu, Z. Phys. **245**, 126 (1971).

²⁷R. Gerhardt, Z. Phys. B: Condens. Matter **22**, 327 (1975).

²⁸A. Manolescu, R. Gerhardt, M. Tornow, D. Weiss, K. von Klitzing, and G. Weinmann, Surf. Sci. **361/362**, 513 (1996).

²⁹M. Tornow, D. Weiss, A. Manolescu, R. Menne, and K. von Klitzing, Phys. Rev. B **54**, 16 397 (1996).

³⁰ $V_0/2$ is also the amplitude of the modulation potential. Here, we avoid this terminology to prevent confusion with the amplitude of $W(x)$ in Eq. (7).